

See discussions, stats, and author profiles for this publication at: <https://www.researchgate.net/publication/332118199>

Study of microstructure and thermal properties of as-cast high carbon and high chromium tool steel

Article in *Metallurgical and Materials Engineering* · March 2019

DOI: 10.30544/392

CITATIONS

2

READS

837

10 authors, including:



Dragan Manasijevic

Technical Faculty in Bor

175 PUBLICATIONS 1,082 CITATIONS

[SEE PROFILE](#)



Zarko Radovic

University of Montenegro

13 PUBLICATIONS 60 CITATIONS

[SEE PROFILE](#)



Nada Štrbac

Technical Faculty in Bor

109 PUBLICATIONS 646 CITATIONS

[SEE PROFILE](#)



Ljubisa Balanovic

University of Belgrade, Technical Faculty in Bor

68 PUBLICATIONS 313 CITATIONS

[SEE PROFILE](#)

Some of the authors of this publication are also working on these related projects:



451-03-68/2020-14/200131 [View project](#)



This work was funded by the Ministry of Science and Technology-Republic of Serbia, the project ON142043 and 142035B as well as the EU project COST MP0602. [View project](#)

STUDY OF MICROSTRUCTURE AND THERMAL PROPERTIES OF AS-CAST HIGH CARBON AND HIGH CHROMIUM TOOL STEEL

Dragan Manasijević^{1}, Žarko Radović², Nada Štrbac¹, Ljubiša Balanović¹,
Uroš Stamenković¹, Milan Gorgievski¹, Duško Minić³, Milena Premović³,
Tamara Holjevac Grgurić⁴, and Nebojša Tadić²*

¹*University of Belgrade, Technical faculty in Bor, VJ12, 19210 Bor, Serbia*

²*University of Montenegro, Faculty of Metallurgy and Technology,
Cetinjski put, bb, 81000, Podgorica, Montenegro*

³*University of Priština, Faculty of Technical Science,
Kneza Miloša 7, 4000 Kosovska Mitrovica, Serbia*

⁴*University of Zagreb, Faculty of Metallurgy,
Aleja narodnih heroja 3, Sisak, Croatia*

Received 03.10.2018

Accepted 10.12.2018

Abstract

This work aims to investigate the microstructural and thermal properties of as-cast high carbon and high chromium cold work tool steel. The microstructure was investigated by using scanning electron microscopy with energy dispersive spectroscopy (SEM-EDS) and X-ray diffraction (XRD) method. It was determined that at room temperature the microstructure of the investigated tool steel includes a lamellar network of M_7C_3 carbide precipitates along grain boundaries of ferrite grains in the base. Thermal diffusivity, specific heat capacity and thermal conductivity of the investigated steel alloy were determined in the temperature interval from 25 to 400 °C by using the laser-flash method. Thermal conductivity increases from 24.9 at 25 °C to 26.9 W/m·K at 400 °C. Phase transition temperatures in the temperature region from room temperature to 1250 °C were experimentally determined using differential scanning calorimetry (DSC). One endothermic effect in the temperature interval from 803 to 820 °C, corresponding to the ferrite/austenite phase transformation, was detected during sample heating. Experimental results were compared with the results of phase equilibria calculations obtained from the ThermoCalc software and TCFE6 database.

Keywords: high alloy tool steel; as-cast; scanning electron microscopy; thermal conductivity; differential scanning calorimetry.

* Corresponding author: Dragan Manasijević, dmanasijevic@tfbor.bg.ac.rs

Introduction

High carbon and high chromium cold work tool steels are extensively used in industry because of their excellent hardenability and high wear resistance [1, 2]. Typical applications of these tool steels include shear blades, trimming and cutting tools, blanking dies, punches, forming and bending rolls [1-3].

High-carbon and high-chromium steels possess excellent abrasion resistance and a high degree of dimensional stability in heat treatment. They are highly resistant to softening at elevated temperatures and moderately resistant to decarburizing and can be nitrided [4].

Although cold work tool steels have been extensively studied in the heat-treated conditions [5-7], investigations of their microstructural and thermal characteristics in as-cast conditions are rare.

The knowledge of microstructure, solidification properties and thermal conductivity of the selected steel should help to improve the design of its structures and components. Thermal conductivity represents an important thermophysical property of material because it controls the size of the temperature gradients which occur in components during their production and use.

In this work microstructure, phase transitions and thermal properties including thermal diffusivity, specific heat and thermal conductivity of the high carbon, high chromium tool steel ingot (165XCrMoW12 (DIN)) were experimentally investigated using: scanning electron microscopy with energy dispersive spectroscopy (SEM-EDS), X-ray powder diffraction (XRD) thermal diffusivity measurements, differential scanning calorimetry (DSC) and thermodynamic calculation of phase equilibria. Obtained results represent a contribution to a better knowledge of microstructural and thermal properties of the investigated high alloy tool steel in its as-cast state.

Experimental procedure

Materials

High carbon and high chromium tool steel was produced in an induction furnace and cast into a standard ingot (60 kg, $t_{\text{cast}} - 1460$ °C). All investigated samples were obtained from the cast ingot. The chemical composition of the investigated samples is given in Table 1.

Table 1. Chemical composition of the investigated tool steel determined by X-ray fluorescence (XRF) technique (in wt.%).

C	Si	Mn	Cr	Ni	Mo	W	V	P	S	Fe
1.65	0.35	0.32	12.5	0.29	0.64	0.45	0.21	0.032	0.029	Balance

Microstructure investigation

Metallographic samples were prepared using conventional grinding and polishing steps and etched at room temperature in 2% Nital reagent for 2-3 s before conducting SEM-EDS. TESCAN VEGA3 scanning electron microscope with energy dispersive spectroscopy (EDS) (Oxford Instruments X-act) was used to observe the microstructure of the investigated steel sample and the measurements were carried out at 20 kV.

Compositions of coexisting phases were determined using EDS area and point analysis. SEM images of the microstructures were taken on the polished and etched surfaces of the studied steel sample in the secondary electron (SE) and back-scatter electrons (BSE) modes.

Identification of co-existing phases was also made using the XRD technique. Powder XRD data were recorded on a D2 PHASER (Bruker, Karlsruhe, Germany) powder diffractometer equipped with a dynamic scintillation detector and ceramic X-ray Cu tube (KFL-Cu-2K) in a 2θ range from 10° to 75° with a step size of 0.02° . The detected XRD pattern was analyzed using ICDD databases PDF2 (2013).

Thermal diffusivity and specific heat measurements

Thermal diffusivity and specific heat were measured using a Discovery Xenon Flash (DXF-500) device. The DXF-500 is equipped with nickel-chrome heaters and an air-cooled aluminum shell. The heating rate was $10^\circ\text{C}/\text{min}$ and the thermal diffusivity measurements were performed within the temperature range from 25 to 400°C in the vacuumed furnace filled with inert gas. Measurement began when the temperature reached a particular value and stayed stable. A liquid nitrogen-cooled IR detector made sample temperature measurements. The steel sample was shaped into a round disk (12.6 mm in diameter and 2 mm thick with plane-parallel ground end faces).

Thermal analysis

Thermal analysis of the investigated steel was carried out using an SDT Q600 (TA Instruments). A sample weighing 50 mg was investigated at a heating rate of $10^\circ\text{C}/\text{min}$ from room temperature up to 1250°C in a nitrogen atmosphere to prevent oxidation. The reference material was an empty alumina crucible.

Results and discussion

Phase equilibria calculation

Thermodynamic calculations of phase equilibria can provide useful information about expected phases, their amounts, and phase transition temperatures [6]. In this work thermodynamic calculation was performed using ThermoCalc software and TCFE6 database [8]. Calculated phase diagram with the labeled composition of the investigated tool steel is shown in Fig. 1. According to the calculated results for the composition of 1.65 wt.% C, upon cooling, solidification starts with the formation of austenite (FCC_A1 phase) at 1392°C . At 1273°C M_7C_3 carbide starts simultaneous crystallization with austenite ($\text{L} \rightarrow \gamma + \text{M}_7\text{C}_3$). Complete solidification of steel is finished at 1256°C . Precipitation of M_{23}C_6 carbide starts at 851°C . Austenite (FCC_A1) to ferrite (BCC_A2) phase transition starts at 809°C and ends at 793°C . At room temperature, the steel microstructure primary consists of ferrite, M_7C_3 , and M_{23}C_6 carbide. However, during rapid solidification of steel metastable supersaturated austenite can be retained in the microstructure [2, 9-11].

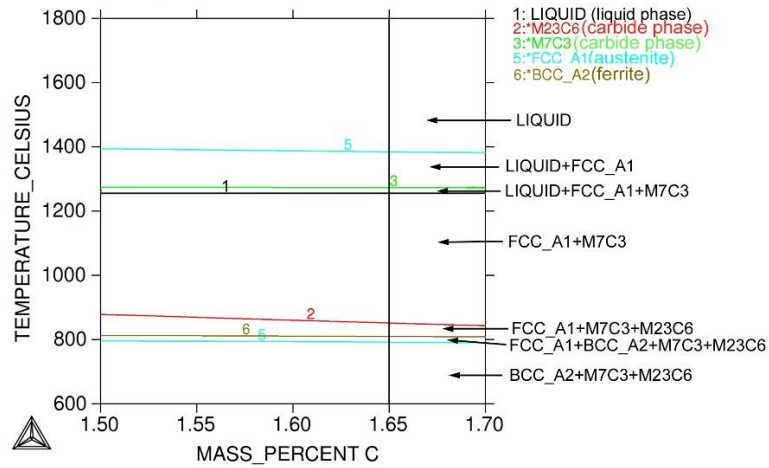


Fig. 1. Calculated pseudo-binary phase diagram of high chromium, high carbon tool steel with the composition of the tool steel (1.65 wt.% C) labeled by a vertical line.

Microstructure investigation

The microstructure of the as-cast high alloy tool steel was investigated using SEM-EDS analysis. Characteristic SEM micrographs of the etched, and polished without etching steel microstructure are shown under different magnifications in Figs. 2a-b and 3a-b.

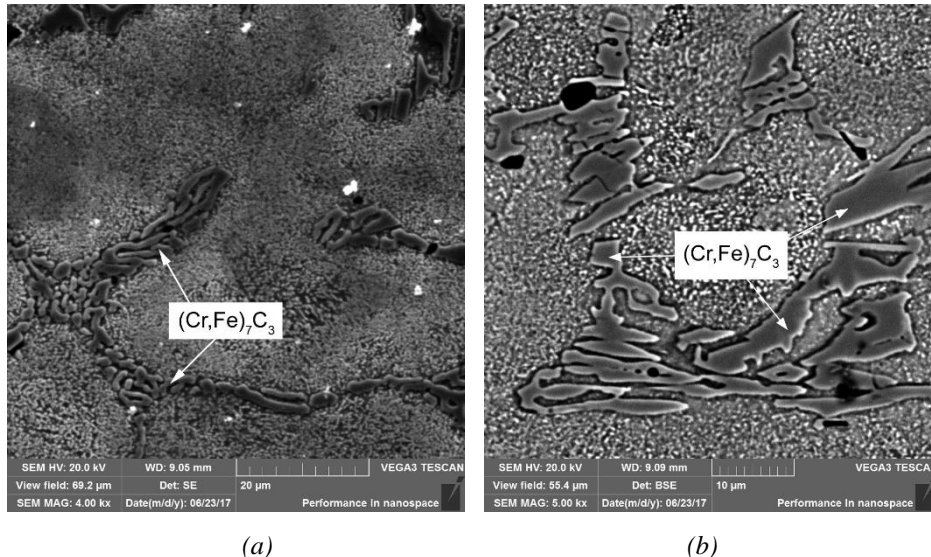


Fig. 2. SEM images of the etched steel microstructure with eutectic carbides network under different magnifications: (a) 4000x; (b) 5000x.

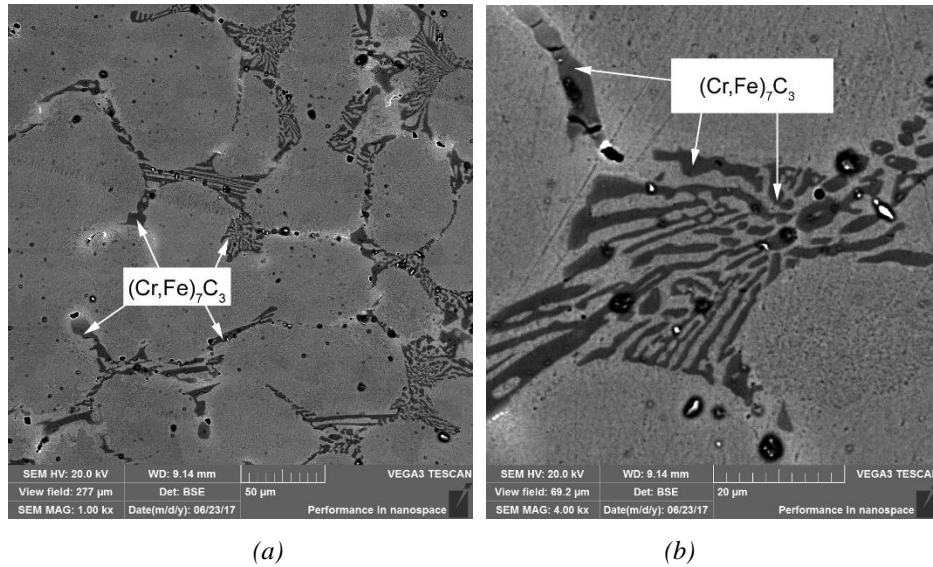


Fig. 3. SEM images of the polished without etching steel microstructure showing the eutectic carbides network under different magnifications: (a) 1000x; (b) 4000x.

Based on the results of SEM-EDS analysis $(\text{Cr, Fe})_7\text{C}_3$ eutectic carbides were identified. In the as-cast sample $(\text{Cr, Fe})_7\text{C}_3$ carbides have precipitated along grain boundaries, forming a continuous carbide network. Secondary M_{23}C_6 carbide precipitates, which were predicted by thermodynamic calculation (Fig. 1), were not observed. The average chemical composition of the identified carbide phase determined by EDS analysis is presented in Table 2.

Table 2. The average chemical composition of the $(\text{Cr, Fe})_7\text{C}_3$ carbide phase determined by EDS analysis with calculated standard uncertainties.

Phase	Average phase composition (at. %)										
	Fe	C	Si	Mn	Cr	Ni	Mo	W	V	P	S
$(\text{Cr,Fe})_7\text{C}_3$	37.0 ± 4.3	28.4 ± 1.0	0.0	0.0	33.3 ± 3.4	0.0	0.0	0.3 ± 0.03	1.0 ± 0.2	0.0	0.0

From Table 2 it could be concluded that the M_7C_3 carbides are mainly composed of Fe, Cr, and C, while small amounts of V and W are also detected.

X-ray diffraction (XRD) was applied to investigate the microstructure of the high alloy tool steel further. The detected XRD pattern for the investigated high alloy tool steel is shown in Fig. 4.

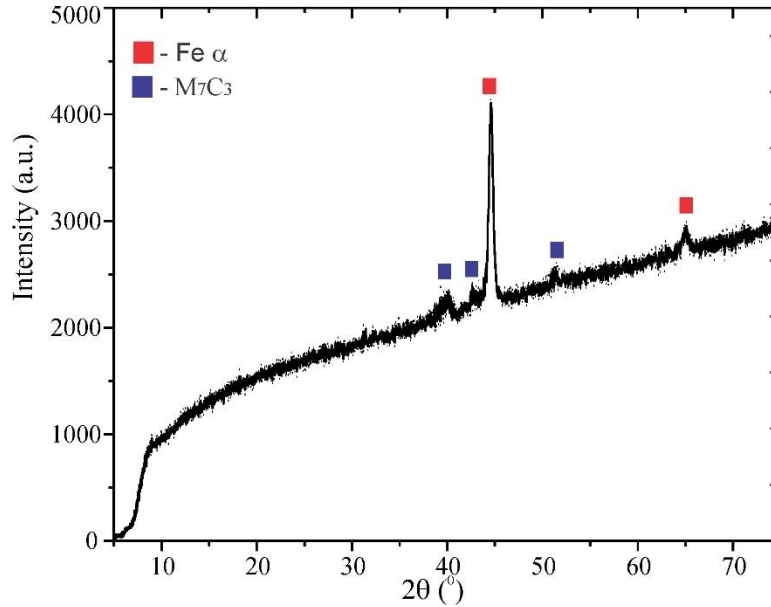


Fig. 4. XRD pattern for the investigated high alloy tool steel.

XRD analysis revealed the presence of ferrite and confirmed the existence of M_7C_3 carbides.

Based on the results of SEM-EDS and XRD analysis it can be concluded that the microstructure of the investigated tool steel primary consists of ferrite and $(Cr, Fe)_7C_3$ carbides which are in general agreement with the result of phase equilibria calculation presented in Fig. 1. Due to the high chromium content, which causes the shifting of the equilibrium Fe-Fe₃C phase diagram to the left, this steel is often called ledeburitic steel. Ledeburitic type of microstructure, represented by the presence of austenitic-carbide eutectic, is frequently found in steels alloyed with strong carbide-forming elements such as Cr, W, V, Nb, and Ti, in which the appropriate alloy carbides replace cementite, often at relatively low alloying element concentrations [12]. It has been reported in the literature that in high carbon, high chromium steels microstructure based on the primary formed an irregular network of eutectic carbides can be modified by applying annealing heat treatment [13] and by addition of modifying elements [14], which leads to the improvement of ductility and impact toughness.

Thermal conductivity measurements

Laser-flash technique [15] is based on uniform irradiation of a disc-shaped sample over its front face with a very short pulse of energy. The sample's thermal diffusivity α is calculated using the following equation [15,16]:

$$\alpha = \frac{1.37L^2}{\pi^2 t_{1/2}} = 0.1388 \frac{L^2}{t_{1/2}} \quad (1)$$

where L represents the thickness of the sample and $t_{1/2}$ is the half-rise time, defined as time interval required for the rear surface temperature to reach half of the maximal temperature increase.

The specific heat capacity C_p of a material represents the amount of energy required to raise a unit mass of the material by one unit of temperature at constant pressure:

$$C_p = \frac{Q}{m\Delta T} \quad (2)$$

where C_p is specific heat capacity (J/kgK), m is mass (kg), ΔT is changed in temperature (K), and Q is the amount of energy (J).

Specific heat capacity can be measured with the laser-flash method by comparing the temperature rise of the sample to the temperature rise of a reference sample of known specific heat capacity, tested under the same conditions [16].

Based on the measured values of the thermal diffusivity and specific heat capacity, the thermal conductivity of the investigated sample can be calculated using a relationship [15]:

$$\lambda = \alpha \cdot \rho \cdot C_p \quad (3)$$

where λ is thermal conductivity (W/mK), α is thermal diffusivity (m^2/s), ρ is density (kg/m^3), and C_p is specific heat capacity (J/kgK).

The calculated values of thermal diffusivity, specific heat capacity and thermal conductivity of the investigated high alloy tool steel in the temperature range from 25 to 400 °C are presented in Table 3.

Table 3. Thermal diffusivity, specific heat capacity and thermal conductivity of the investigated high alloy steel in the temperature interval from 25 to 400 °C.

Temperature (°C)	Thermal diffusivity (cm^2/s)	Specific heat capacity (J/kg·K)	Thermal conductivity (W/m·K)
25	0.0623	518.1329	24.9258
100	0.0620	526.8658	25.2216
200	0.0609	556.4617	26.1615
300	0.0590	581.0959	26.4783
400	0.0561	621.7637	26.9317

Temperature dependence of thermal conductivity for the investigated high alloy tool steel is graphically presented in Fig. 5.

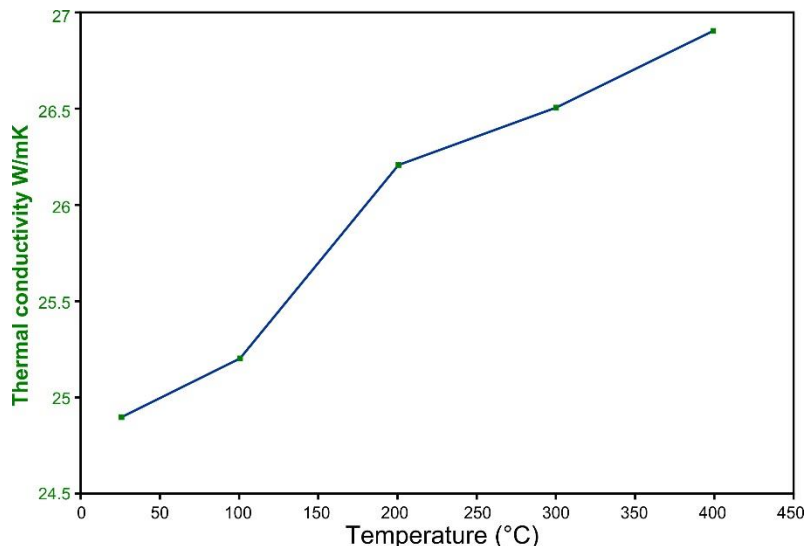


Fig. 5. Temperature dependence of thermal conductivity for the investigated high alloy tool steel in the temperature range from 25 to 400 °C.

From Table 3 it can be seen that, in the investigated temperature interval, thermal diffusivity decreases and specific heat capacity increases with increasing temperature. The thermal conductivity of the investigated tool steel consistently increases from 24.9 W/m·K at 25 °C to 26.9 W/m·K at 400 °C. These low values of thermal conductivity are to be expected for high alloy steels [17]. It is a well-established fact that at ambient temperature, high alloy steels have much lower thermal conductivity compared to the cast irons and carbon steels due to the large number of alloying elements [17, 18]. Pure iron has the highest value of thermal conductivity followed by carbon steels, alloy steels and then by high alloy steels [16-18]. However, with an increase in temperature the thermal conductivities of irons and low alloyed steels decrease, while the conductivities of high alloy steels increase as is shown in Fig. 5 [17, 18].

Thermal analysis

Phase transition temperatures of the investigated steel were investigated using DSC heating curves in the temperature interval from 25 to 1250 °C with the heating rate of 10 °C/min. Only one endothermic effect was identified during heating of the investigated steel sample (Fig. 6). The extrapolated onset temperature of the identified peak was 803.5 °C, the peak maximum temperature was 814.3 °C, and the end of the peak was at 820.5 °C. According to the results of phase equilibria calculation shown in Fig. 1 the thermal interval of ferrite/austenite phase transformation is from 809 to 793 °C; therefore the identified thermal endothermic effect can be considered as phase transformation of ferrite to austenite. The measured temperature of the solid-state phase transformation is in good agreement with the experimental result of *Bombac et al.* [6] and somewhat lower than experimentally determined temperature by *Moravčík et al.* [19].

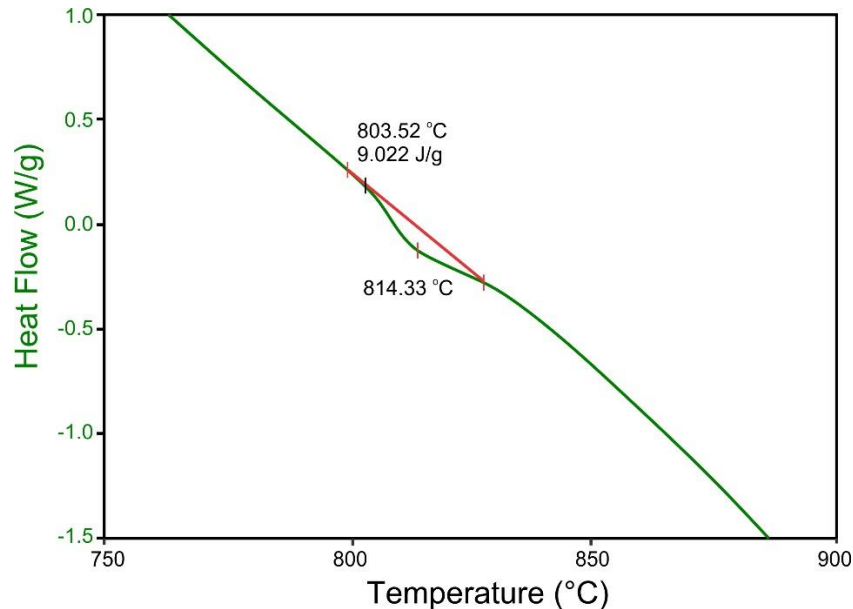


Fig. 6. Part of the DSC heating curve for the investigated sample of the high alloy tool steel with the endothermic effect in the temperature range from 803 to 820 °C.

Conclusions

Microstructure and thermal properties of high carbon, high chromium tool steel in the as-cast state were investigated in this work. Based on the results presented in this paper it can be concluded that the investigated tool steel shows a ledeburitic type of microstructure with M_7C_3 austenitic-carbide eutectics network along the grain boundaries of the matrix phase. The precipitated M_7C_3 carbides have a lamellar shape and are composed mainly of Fe, Cr and C. Experimentally determined temperature dependence of thermal conductivity in the temperature interval from 25 to 400 °C show a consistent increase from 24.9 to 26.9 W/m·K. One endothermic effect in the temperature interval from 803 to 820 °C, is contributed to the ferrite/austenite phase transition and at temperatures below 800 °C austenite is wholly converted into ferrite and carbides.

Acknowledgments

This study was done in the frame of the bilateral project between the University of Belgrade, Technical Faculty in Bor (Serbia) and University of Podgorica, Faculty of Metallurgy and Technology (Montenegro) entitled "Investigation of thermal, structural and mechanical properties of high alloy tool steels".

References

- [1] G. Roberts, G. Krauss, R. Kennedy: Tool Steels, Materials Park: ASM International, 1998.
- [2] J. Valloton, D. M. Herlach, H. Henein, D. Sediako: Metall Mat Trans A, 48 (10) (2017) 4735-4743.
- [3] T. Večko Pirtovšek, G. Kugler, M. Terčelj: Mater Charact, 83 (2013) 97-108.
- [4] T. Packiaraj Rajendran, N. Rajesh Jesudoss Hynes, T. Christopher: J Braz Soc Mech Sci Eng, 40 (2018) Article: 316.
- [5] T. Amine, J W. Newkirk, H. El-Din, F. El-Sheikh, F. Liou: Int J Adv Manuf Technol, 73 (9-12) (2014) 1427-1435.
- [6] D. Bombac, M. Fazarinc, A. Saha Podder, G. Kugler: J Mater Eng Perform, 22 (3) (2013) 742-747.
- [7] H. Torkamani, Sh. Raygan, J. Rassizadehghani: Mater Design, 54 (2014) 1049-1055.
- [8] J. O. Andersson, T. Helander, L. Höglund, P. Shi, B. Sundman: Calphad, 26 (2) (2002) 273-312.
- [9] D. Aišman, H. Jirkova, B. Mašek: J Alloy Compd, 536 (2012) S204-S207.
- [10] M. N. Mohammed, M. Z. Omar, J. Syarif, Z. Sajuri, M. S. Salleh, K. S. Alhawari, The Scientific World Journal, Article ID 828926, (2013), 7 pages.
- [11] S. Kahrobaee, M. Kashefi: J Mater Eng Perform, 24 (3) (2015) 1192-1198.
- [12] E. C. Bain: Alloying Elements in Steels, ASM, Cleveland, Ohio, USA, 1939.
- [13] G. Ramesh, R. Rahul, M. Pradeep, P. Sreehari, S. Ramesh Kumar: Materials Today: Proceedings, 5 (2018) 2733-2737.
- [14] M.A. Hamidzadeh, M. Meratian, M. Mohammadi Zahrani: Mat Sci Eng A-Struct, 556 (2012) 758-766.
- [15] W. J. Parker, R. J. Jenkins, C. P. Butler, G. L. Abbott: J Appl Phys, 32 (9) (1961) 1679.
- [16] D. Manasijević, Ž. Radović, N. Štrbac, Lj. Balanović, U. Stamenković, M. Gorgievski, M. Premović, T. Holjevac Grgurić, N. Tadić: Mater Test, 60 (12) (2018) 1175-1178.
- [17] S. M. Shelton: Bureau of Standards Journal of Research, 12 (1934) 441.
- [18] M. J. Peet, H. S. Hasan, H. K. D. H. Bhadeshia: Int J Heat Mass Tran, 54 (11-12) (2011) 2602-2608.
- [19] R. Moravčík, M. Štefániková, R. Čička, E. Čaplovič, K. Kocúrová, R. Šturm: Strojníški vestnik - Journal of Mechanical Engineering, 58 (12) (2012) 709-715.



Creative Commons License

This work is licensed under a Creative Commons Attribution 4.0 International License.